

1 Inferring the effective start dates of non-pharmaceutical  
2 interventions during COVID-19 outbreaks

3 Ilia Kohanovski<sup>1</sup>, Uri Obolski<sup>2,3</sup>, and Yoav Ram<sup>1,a</sup>

4 <sup>1</sup>School of Computer Science, Interdisciplinary Center Herzliya, Herzliya 4610101, Israel

5 <sup>2</sup>School of Public Health, Tel Aviv University, Tel Aviv 6997801, Israel

6 <sup>3</sup>Porter School of the Environment and Earth Sciences, Tel Aviv University, Tel Aviv 6997801, Israel

7 <sup>a</sup>Corresponding author: yoav@yoavram.com

8 May 21, 2020

9 **Abstract**

10 During February and March 2020, several countries implemented non-pharmaceutical inter-  
11 ventions, such as school closures and lockdowns, with variable schedules to control the COVID-19  
12 pandemic caused by the SARA-CoV-2 virus. Overall, these interventions seem to have success-  
13 fully reduced the spread of the pandemic. We hypothesize that the official and effective start  
14 date of such interventions can significantly differ, for example due to slow diffusion of guidelines  
15 in the population, or due to unpreparedness of the authorities and the public. We use an SEIR  
16 epidemiological model and an MCMC inference framework to estimate the effective start of NPIs  
17 in several countries, and compare these effective dates to the official dates. We report our finding  
18 of both late and early effects of NPIs, and discuss potential causes and consequences of our results.

## 19 Introduction

20 The COVID-19 pandemic has resulted in implementation of extreme non-pharmaceutical interventions  
21 (NPIs) in many affected countries. These interventions, from social distancing to lockdowns, are  
22 applied in a rapid and widespread fashion. The NPIs are designed and assessed using epidemiological  
23 models, which follow the dynamics of the viral infection to forecast the effect of different mitigation and  
24 suppression strategies on the levels of infection, hospitalization, and fatality. These epidemiological  
25 models usually assume that the effect of NPIs on disease transmission begins at the officially declared  
26 date (e.g. (author?)<sup>1,2,3</sup>).

27 Adoption of public health recommendations is often critical for effective response to infectious dis-  
28 eases, and has been studied in the context of HIV<sup>4</sup> and vaccination<sup>5,6</sup>, for example. However,  
29 behavioral and social change does not occur immediately, but rather requires time to diffuse in the  
30 population through media, social networks, and social interactions. Moreover, compliance to NPIs  
31 may differ between different interventions and between people. For example, in a survey of 2,108  
32 adults in the UK during Mar 2020, (author?)<sup>7</sup> found that those over 70 years old were more likely to  
33 adopt social distancing than young adults (18-34 years old), and that those with lower income were  
34 less likely to be able to work from home and to self-isolate. Similarly, compliance to NPIs may be  
35 impacted by personal experiences. (author?)<sup>8</sup> have surveyed 6,149 UK adults in late April and found  
36 that people who believe they have already had COVID-19 are more likely to think they are immune,  
37 and less likely to comply with social distancing measures. Compliance may also depend on risk  
38 perception as perceived by the the number of domestic cases or even by reported cases in other regions  
39 and countries. Interestingly, the perceived risk of COVID-19 infection has likely caused a reduction  
40 in the number of influenza-like illness cases in the US starting from mid-February<sup>9</sup>.

41 Here, we hypothesize that there is a significant difference between the official start of NPIs and their  
42 adoption by the public and therefore their effect on transmission dynamics. We use a *Susceptible-*  
43 *Exposed-Infected-Recovered* (SEIR) epidemiological model and *Markov Chain Monte Carlo* (MCMC)  
44 parameter estimation framework to estimate the effective start date of NPIs from publicly available  
45 COVID-19 case data in several geographical regions. We compare these estimates to the official dates  
46 and find both late and early effects of NPIs on COVID-19 transmission dynamics. We conclude by  
47 demonstrating how differences between the official and effective start of NPIs can confuse assessments  
48 of the effectiveness of the NPIs in a simple epidemic control framework.

## 49 Models and Methods

50 **Data.** We use daily confirmed case data  $\mathbf{X} = (X_1, \dots, X_T)$  from several different countries. These  
51 incidence data summarize the number of individuals  $X_t$  tested positive for SARS-CoV-2 RNA (using  
52 RT-qPCR) at each day  $t$ . Data for Wuhan, China retrieved from (author?)<sup>10</sup>, data for 11 European  
53 countries retrieved from (author?)<sup>3</sup>. Regions in which there were multiple sequences of days with  
54 zero confirmed cases (e.g. France), we cropped the data to begin with the last sequence so that our  
55 analysis focuses on the first sustained outbreak rather than isolated imported cases. For dates of official  
56 NPI dates see Table 1.

57 **SEIR model.** We model SARS-CoV-2 infection dynamics by following the number of susceptible  
58  $S$ , exposed  $E$ , reported infected  $I_r$ , and unreported infected  $I_u$  individuals in a population of size  $N$ .  
59 This model distinguishes between reported and unreported infected individuals: the reported infected  
60 are those that have enough symptoms to eventually be tested and thus appear in daily case reports, to  
61 which we fit the model.

Country	First	Last
Austria	Mar 10 2020	Mar 16 2020
Belgium	Mar 12 2020	Mar 18 2020
Denmark	Mar 12 2020	Mar 18 2020
France	Mar 13 2020	Mar 17 2020
Germany	Mar 12 2020	Mar 22 2020
Italy	Mar 5 2020	Mar 11 2020
Norway	Mar 12 2020	Mar 24 2020
Spain	Mar 9 2020	Mar 14 2020
Sweden	Mar 12 2020	Mar 18 2020
Switzerland	Mar 13 2020	Mar 20 2020
United Kingdom	Mar 16 2020	Mar 24 2020
Wuhan	Jan 23 2020	Jan 23 2020

**Table 1: Official start of non-pharmaceutical interventions.** The date of the first intervention is for a ban of public events, or encouragement of social distancing, or for school closures. In all countries except Sweden, the date of the last intervention is for a lockdown. In Sweden, where a lockdown was not ordered during the studied dates, the last date is for school closures. Dates for European countries from (author?)<sup>3</sup>, date for Wuhan, China from (author?)<sup>10</sup>. See Figure 1 for a visual presentation.

62 Susceptible ( $S$ ) individuals become exposed due to contact with reported or unreported infected  
 63 individuals ( $I_r$  or  $I_u$ ) at a rate  $\beta_t$  or  $\mu\beta_t$ . The parameter  $0 < \mu < 1$  represents the decreased transmission  
 64 rate from unreported infected individuals, who are often subclinical or even asymptomatic. The  
 65 transmission rate  $\beta_t \geq 0$  may change over time  $t$  due to behavioral changes of both susceptible and  
 66 infected individuals. Exposed individuals, after an average incubation period of  $Z$  days, become  
 67 reported infected with probability  $\alpha_t$  or unreported infected with probability  $(1 - \alpha_t)$ . The reporting  
 68 rate  $0 < \alpha_t < 1$  may also change over time due to changes in human behavior. Infected individuals  
 69 remain infectious for an average period of  $D$  days, after which they either recover, or becomes ill  
 70 enough to be quarantined. They therefore no longer infect other individuals, and the model does not  
 71 track their frequency. The model is described by the following equations:

$$\begin{aligned}
 \frac{dS}{dt} &= -\beta_t S \frac{I_r}{N} - \mu\beta_t S \frac{I_u}{N} \\
 \frac{dE}{dt} &= \beta_t S \frac{I_r}{N} + \mu\beta_t S \frac{I_u}{N} - \frac{E}{Z} \\
 \frac{dI_r}{dt} &= \alpha_t \frac{E}{Z} - \frac{I_r}{D} \\
 \frac{dI_u}{dt} &= (1 - \alpha_t) \frac{E}{Z} - \frac{I_r}{D}.
 \end{aligned} \tag{1}$$

72  
 73 The initial numbers of exposed  $E(0)$  and unreported infected  $I_u(0)$  are considered model parameters,  
 74 whereas the initial number of reported infected is assumed to be zero  $I_r(0) = 0$ , and the number of  
 75 susceptible is  $S(0) = N - E(0) - I_u(0)$ . This model is inspired by (author?)<sup>1</sup> and (author?)<sup>10</sup>, who  
 76 used a similar model with multiple regions and constant transmission  $\beta$  and reporting rate  $\alpha$  to infer  
 77 COVID-19 dynamics in China and the continental US, respectively.

78 **Likelihood function.** For a given vector  $\theta$  of model parameters the *expected* cumulative number of  
 79 reported infected individuals ( $I_r$ ) until day  $t$  is, following Eq. (1),

$$80 \quad Y_t(\theta) = \int_0^t \alpha_s \frac{E(s)}{Z} ds, \quad Y_0 = 0. \tag{2}$$

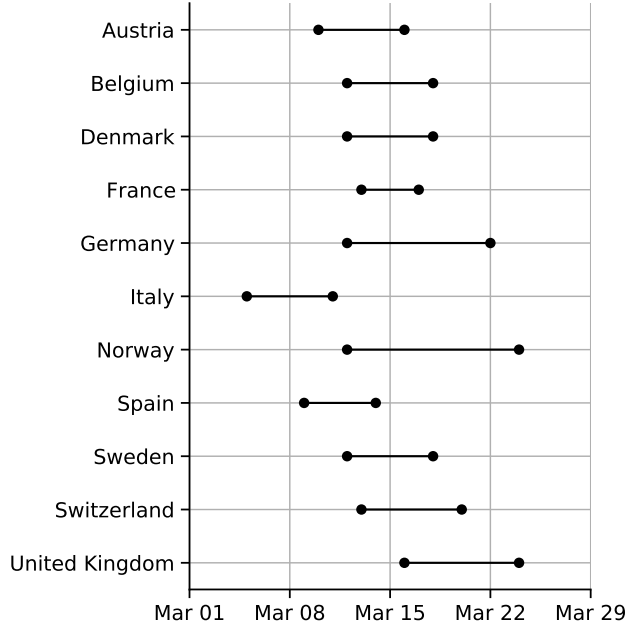


**Figure 1: Official start of non-pharmaceutical interventions.** See Table 1 for more details. Wuhan, China is not shown.

We assume that reported infected individuals are confirmed and therefore observed in the daily case report of day  $t$  with probability  $p_t$  (note that an individual can only be observed once, and that  $p_t$  may change over time, but  $t$  is a specific date rather than the time elapsed since the individual was infected). We denote by  $X_t$  the number of confirmed cases in day  $t$ , and by  $\tilde{X}_t$  the cumulative number of confirmed cases until day  $t$ ,

$$\tilde{X}_t = \sum_{i=1}^t X_i. \quad (3)$$

Therefore, at day  $t$  the number of reported infected yet-to-be confirmed individuals is  $(Y_t(\theta) - \tilde{X}_{t-1})$ . We therefore assume that  $X_t$  conditioned on  $\tilde{X}_{t-1}$  is Poisson distributed,

$$\begin{aligned} (X_1 | \theta) &\sim Poi(Y_1(\theta) \cdot p_1), \\ (X_t | \tilde{X}_{t-1}, \theta) &\sim Poi((Y_t(\theta) - \tilde{X}_{t-1}) \cdot p_t), \quad t > 1. \end{aligned} \quad (4)$$

Hence, the *likelihood function*  $\mathbb{L}(\theta | \mathbf{X})$  for the parameter vector  $\theta$  given the confirmed case data  $\mathbf{X} = (X_1, \dots, X_T)$  is defined by the probability to observe  $\mathbf{X}$  given  $\theta$ ,

$$\mathbb{L}(\theta | \mathbf{X}) = P(\mathbf{X} | \theta) = P(X_1 | \theta) \cdot P(X_2 | \tilde{X}_1, \theta) \cdots P(X_T | \tilde{X}_{T-1}, \theta). \quad (5)$$

**NPI model.** To model non-pharmaceutical interventions (NPIs), we set the beginning of the NPIs to day  $\tau$  and define

$$\beta_t = \begin{cases} \beta, & t < \tau \\ \beta\lambda, & t \geq \tau \end{cases}, \quad \alpha_t = \begin{cases} \alpha_1, & t < \tau \\ \alpha_2, & t \geq \tau \end{cases}, \quad p_t = \begin{cases} 1/9, & t < \tau \\ 1/6, & t \geq \tau \end{cases}, \quad (6)$$

where  $0 < \lambda < 1$ . The values for  $p_t$  follow (author?)<sup>1</sup>, who estimated the average time between infection and reporting in Wuhan, China, at 9 days before the start of NPIs and 6 days after start of NPIs.

99 **Parameter estimation.** To estimate the model parameters from the daily case data  $\mathbf{X}$ , we apply a  
 100 Bayesian inference approach. We start our model  $\Delta t$  days<sup>2</sup> before the outbreak (defined as consecutive  
 101 days with increasing confirmed cases) in each country. The model in Eq. (1) is parameterized by the  
 102 vector  $\theta$ , where

103 
$$\theta = (Z, D, \mu, \{\beta_t\}, \{\alpha_t\}, \{p_t\}, E(0), I_u(0), \tau, \Delta t). \quad (7)$$

104 The likelihood function is defined in Eq. (5). The posterior distribution of the model parameters  
 105  $P(\theta | \mathbf{X})$  is estimated using an *affine-invariant ensemble sampler for Markov chain Monte Carlo*  
 106 (MCMC)<sup>11</sup> implemented in the `emcee` Python package<sup>12</sup>.

107 We defined the following prior distributions on the model parameters  $P(\theta)$ :

$$\begin{aligned} Z &\sim Uniform(2, 5) \\ D &\sim Uniform(2, 5) \\ \mu &\sim Uniform(0.2, 1) \\ \beta &\sim Uniform(0.8, 1.5) \\ \lambda &\sim Uniform(0, 1) \\ \alpha_1, \alpha_2 &\sim Uniform(0.02, 1) \\ E(0) &\sim Uniform(0, 3000) \\ I_u(0) &\sim Uniform(0, 3000) \\ \Delta t &\sim Uniform(1, 5) \\ \tau &\sim TruncatedNormal\left(\frac{\tau^* + \tau^0}{2}, \frac{\tau^* - \tau^0}{2}, 1, T - 2\right), \end{aligned} \quad (8)$$

109 where the prior for  $\tau$  is a truncated normal distribution shaped so that the date of the first and last NPI,  
 110  $\tau^0$  and  $\tau^*$  (Table 1), are at minus and plus one standard deviation, and taking values only between  
 111 1 and  $T - 2$ , where  $T$  is the number of days in the data  $\mathbf{X}$ . We have also tested an uninformative  
 112 uniform prior  $U(1, T - 2)$ . The uninformative prior could result in non-negligible posterior probability  
 113 for unreasonable  $\tau$  values, such as Mar 1 in the United Kingdom. This was probably due to MCMC  
 114 chains being stuck in low posterior regions of the parameter space. We therefore decided to use  
 115 the more informative truncated normal prior. Other priors follow (**author?**)<sup>1</sup>, with the following  
 116 exceptions.  $\lambda$  is used to ensure transmission rates are lower after the start of the NPIs ( $\lambda < 1$ ). We  
 117 checked values of  $\Delta t$  larger than five days and found they generally produce lower likelihood, higher  
 118 DIC (see below), and unreasonable parameter estimates, and therefore chose  $U(1, 5)$  as the prior.

119 **Model comparison.** We perform model selection using two methods. First, we compute WAIC  
 120 (widely applicable information criterion)<sup>13</sup>,

121 
$$WAIC(\theta, \mathbf{X}) = -2 \log \mathbb{E}[\mathcal{L}(\theta | \mathbf{X})] + 2\mathbb{V}[\log \mathcal{L}(\theta | \mathbf{X})] \quad (9)$$

122 where  $\mathbb{E}[\cdot]$  and  $\mathbb{V}[\cdot]$  are the expectation and variance operators taken over the posterior distribution  
 123  $P(\theta | \mathbf{X})$ . We compare models by reporting their relative WAIC; lower is better (Table 2). A minority  
 124 of MCMC chains that fail to fully converge can lead to overestimation of the variance (the second  
 125 term in Eq. (9)). Therefore, we exclude from the WAIC computation chains with mean log-likelihood  
 126 that is three standard deviations or more from the overall mean.

127 We also apply posterior predictive plots, in which we sample 1,000 parameter vectors from the  
 128 posterior distributions  $P(\theta | \mathbf{X})$  and use them to simulate the SEIR model (Eq. (1)). We plot these  
 129 simulated dynamics together with the data (Figure S3a). Both the accuracy (i.e. overlap of data  
 130 and prediction) and the precision (i.e. the compactness of the predictions) are good ways to visually  
 131 compare models.

132 **Source code.** We use Python 3 with the NumPy, Matplotlib, SciPy, Pandas, Seaborn, and emcee  
 133 packages. All source code will be publicly available under a permissive open-source license at  
 134 [github.com/yoavram-lab/EffectiveNPI](https://github.com/yoavram-lab/EffectiveNPI). Files containing samples from the posterior distributions will  
 135 be deposited on FigShare.

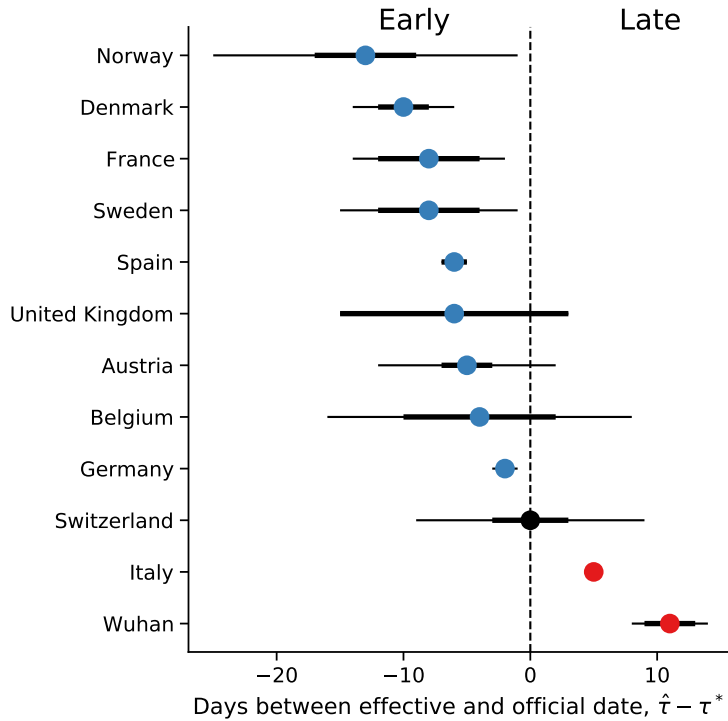


**Figure 2: Official and effective start of non-pharmaceutical interventions.** The difference between  $\hat{\tau}$  the effective and  $\tau^*$  the official start of NPI is shown for different regions. The effective NPI dates in Italy and Wuhan are significantly delayed compared to the official dates, whereas in Denmark, France, Spain, and Germany, the effective date is earlier than the official date.  $\hat{\tau}$  is the posterior median, see Table 3.  $\tau^*$  is the last NPI date, see Table 1. Thin and bold lines show 95% and 75% credible intervals, respectively (area in which  $P(|\tau - \hat{\tau}| \mid \mathbf{X}) = 0.95$  and 0.75.)

## 136 Results

137 Several studies have described the effects of non-pharmaceutical interventions in different geographical  
 138 regions<sup>3;2;1</sup>. These studies have assumed that the parameters of the epidemiological model change at  
 139 a specific date, as in Eq. (6), and set the change date  $\tau$  to the official NPI date  $\tau^*$  (Table 1). They  
 140 then fit the model once for time  $t < \tau^*$  and once for time  $t \geq \tau^*$ . For example, (**author?**)<sup>1</sup> estimate  
 141 the dynamics in China before and after  $\tau^*$  at Jan 23. Thereby, they effectively estimate  $(\beta, \alpha_1)$  and  
 142  $(\lambda, \alpha_2)$  separately. Here we estimate the posterior distribution  $P(\tau \mid \mathbf{X})$  of the *effective* start date of the  
 143 NPIs by jointly estimating  $\tau, \beta, \lambda, \alpha_1, \alpha_2$  on the entire data per region (e.g. Italy, Austria), rather than  
 144 splitting the data at  $\tau^*$ . We then estimate the posterior probability  $P(\tau \mid \mathbf{X})$  by marginalizing the joint  
 145 posterior, and estimate  $\hat{\tau}$  as the posterior median.

146 We compared the posterior predictive plots of a model with a free  $\tau$  with those of a model with  $\tau$  fixed  
 147 at  $\tau^*$  and without  $\tau$ . The model with free  $\tau$  clearly produces better and less variable predictions (Figure S3a). When we compared the models using WAIC (Table 2), the model with a free parameter for  
 148 the start of the NPI was better than the other models in 8 out of 12 of the regions; the exceptions are  
 149 Austria, Belgium, Norway, and United Kingdom.

151 We compare the official  $\tau^*$  and effective  $\hat{\tau}$  start of NPIs and find that in most regions the effective start  
 152 of NPI significantly differs from the official date (Figure 2);; that is, the credible interval on  $\hat{\tau}$  does  
 153 not include  $\tau^*$  (Figure 2). The exceptions are, as with the comparison to the simpler models, Austria,  
 154 Belgium, and United Kingdom, as well another country (see below). Norway also has a relatively  
 155 wide credible interval, which could be expected as it has the longest duration between the first and last  
 156 NPIs (Table 1). In the following, we describe our findings on late and early effective start of NPI in  
 157 detail.

Country	Fixed	Free	No
Austria	26.68	28.40	39.70
Belgium	29.38	30.62	28.80
Denmark	38.56	<b>37.34</b>	49.63
France	49.90	<b>49.60</b>	72.17
Germany	214.95	<b>158.90</b>	310.65
Italy	301.39	<b>233.07</b>	433.42
Norway	34.04	36.07	37.54
Spain	59.93	<b>59.54</b>	141.96
Sweden	25.93	<b>25.91</b>	28.35
Switzerland	74.90	<b>72.97</b>	99.65
United Kingdom	38.10	37.39	35.77
Wuhan China	94.00	<b>73.75</b>	107.31

**Table 2: WAIC values for the different models.** WAIC (widely applicable information criterion)<sup>13</sup> values for models with: no  $\tau$  at all, *No*;  $\tau$  fixed at the official last NPI date  $\tau^*$ , *Fixed*; and free parameter  $\tau$ , *Free*. WAIC values are scaled as a deviance measure: lower values imply higher predictive accuracy.

158 **Late effective start of NPIs.** In both Wuhan, China, and in Italy we find that our estimated effective  
 159 start of NPI  $\hat{\tau}$  is significantly later than the official date  $\tau^*$  (Figure 2).

160 In Italy, the first case was officially confirmed on Feb 21. School closures were implemented on  
 161 Mar 5<sup>3</sup>, a lockdown was declared in Northern Italy on Mar 8, with social distancing implemented in  
 162 the rest of the country, and the lockdown was extended to the entire nation on Mar 11<sup>2</sup>. That is, the  
 163 first and last official dates are Mar 8 and Mar 11. However, we estimate the effective date  $\hat{\tau}$  at Mar 16  
 164 ( $\pm 0.47$  days 95% CI ; Figure 3).

165 Similarly, in Wuhan, China, a lockdown was ordered on Jan 23<sup>1</sup>, but we estimate the effective start of  
 166 NPIs to be several days later at Feb 2 ( $\pm 2.85$  days 95% CI Figure 3).

167 **Early effective start of NPIs.** In contrast, in some regions we estimate an effective start of NPIs  $\hat{\tau}$   
 168 that is *earlier* than the official date  $\tau^*$  (Figure 2). In Spain, social distancing was encouraged starting  
 169 on Mar 8<sup>3</sup>, but mass gatherings still occurred on Mar 8, including a march of 120,000 people for the  
 170 [International Women's Day](#), and a football match between [Real Betis](#) and [Real Madrid](#) (2:1) with a  
 171 crowd of 50,965 in Seville. A national lockdown was only announced on Mar 14<sup>3</sup>. Nevertheless, we  
 172 estimate the effective start of NPI  $\hat{\tau}$  on Mar 8 or 9 ( $\pm 1.08$  95%CI), rather than Mar 14 (Figure 4).

173 Similarly, in France we estimate the effective start of NPIs  $\hat{\tau}$  on Mar 8 or Mar 9 ( $\pm 6.27$  days 95% CI,  
 174 Figure 4). Although the credible interval is wider compared to Spain, spanning from Mar 2 to Mar 15,  
 175 the official lockdown start at Mar 17 is later still, and even the earliest NPI, banning of public events,  
 176 only started on Mar 13<sup>3</sup>.

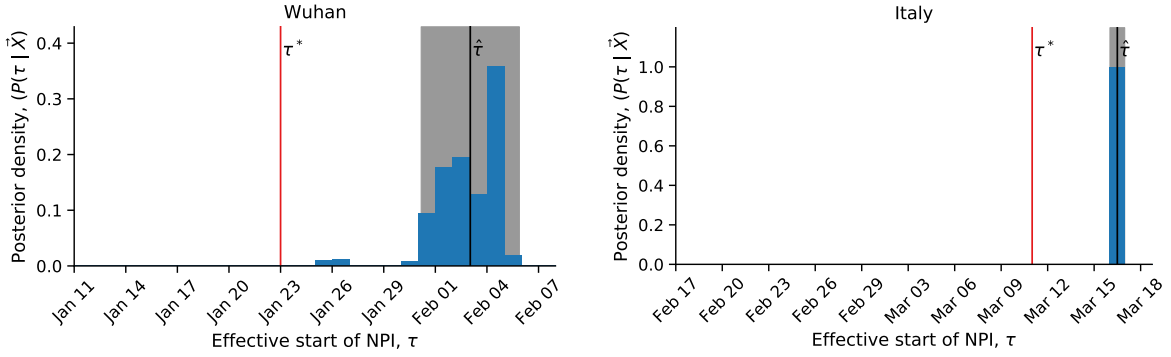


**Figure 3: Late effect of non-pharmaceutical interventions in Italy and Wuhan, China.** Posterior distribution of  $\tau$ , the effective start date of NPI, is shown as a histogram of MCMC samples. Red line shows the official last NPI date  $\tau^*$ . Black line shows the estimated  $\hat{\tau}$ . Shaded area shows a 95% credible interval (area in which  $P(|\tau - \hat{\tau}| \mid \mathbf{X}) = 0.95$ ).

177 Interestingly, the effective start of NPIs  $\hat{\tau}$  in both France and Spain is estimated at Mar 8, although  
 178 the official NPI dates differ significantly: the first NPI in France is only one day before the last NPI in  
 179 Spain. The number of daily cases was similar in both countries until Mar 8, but diverged by Mar 13,  
 180 reaching significantly higher numbers in Spain (Figure S1). This may suggest that correlation exist  
 181 between effective start of NPIs due to global or international events.

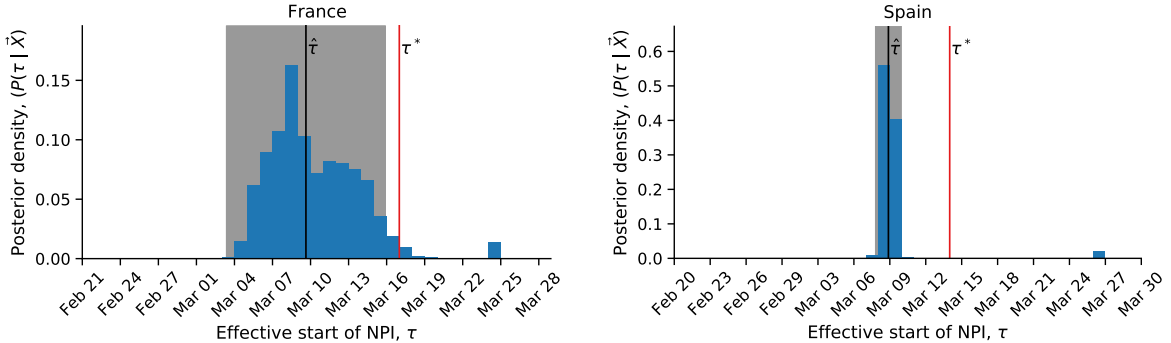


**Figure 4: Early effect of non-pharmaceutical interventions in France and Spain.** Posterior distribution of  $\tau$ , the effective start date of NPI, is shown as a histogram of MCMC samples. Red line shows the official last NPI date  $\tau^*$ . Black line shows the estimated  $\hat{\tau}$ . Shaded area shows a 95% credible interval (area in which  $P(|\tau - \hat{\tau}| \mid \mathbf{X}) = 0.95$ ).

182 **Like a Swiss watch.** We find one case in which the official and effective dates match: Switzerland  
 183 ordered a national lockdown on Mar 20, after banning public events and closing schools on Mar 13  
 184 and 14<sup>3</sup>. Indeed, the posterior median  $\hat{\tau}$  is Mar 20 ( $\pm 8.46$  days 95% CI), and the posterior distribution  
 185 shows two density peaks: a smaller one between Mar 10 and Mar 14, and a bigger one between Mar 17  
 186 and Mar 22 (Figure S2). It's also worth mentioning that Switzerland was the first to mandate self  
 187 isolation of confirmed cases<sup>3</sup>.

Country	$\tau^*$	$\tau$	$CI_{75\%}$	$CI_{95\%}$	$Z$	$D$	$\mu$	$\beta$	$\alpha_1$	$\lambda$	$\alpha_2$	$E(0)$	$I_u(0)$	$\Delta t$
Austria	Mar 16	Mar 11	2.0	7.0	3.92	3.59	0.43	1.10	0.06	0.73	0.45	464.24	555.98	2.0
Belgium	Mar 18	Mar 14	6.0	12.0	3.95	3.56	0.43	1.09	0.22	0.84	0.43	364.73	464.54	2.0
Denmark	Mar 18	Mar 08	2.0	4.0	3.96	3.47	0.37	1.06	0.04	0.32	0.53	501.86	638.74	2.0
France	Mar 17	Mar 09	4.0	6.0	4.00	3.70	0.56	1.14	0.20	0.66	0.45	530.90	607.66	1.0
Germany	Mar 22	Mar 20	0.0	1.0	3.77	4.05	0.75	1.21	0.30	0.80	0.12	178.64	112.04	2.0
Italy	Mar 11	Mar 16	0.0	0.0	4.16	2.79	0.50	1.00	0.53	0.46	0.53	935.34	1928.88	1.0
Norway	Mar 24	Mar 11	4.0	12.0	4.04	3.46	0.41	1.07	0.13	0.68	0.27	353.40	486.72	2.0
Spain	Mar 14	Mar 08	1.0	1.0	3.94	3.62	0.61	1.11	0.07	0.73	0.53	898.03	897.61	2.0
Sweden	Mar 18	Mar 10	4.0	7.0	4.02	3.50	0.42	1.06	0.11	0.64	0.25	386.21	494.37	2.0
Switzerland	Mar 20	Mar 20	3.0	9.0	3.95	3.74	0.62	1.11	0.18	0.47	0.21	203.22	230.43	2.0
United Kingdom	Mar 24	Mar 18	9.0	9.0	3.98	3.82	0.54	1.15	0.21	0.83	0.39	268.76	260.68	2.0
Wuhan, China	Jan 23	Feb 03	2.0	3.0	3.73	3.63	0.61	1.15	0.28	0.18	0.35	597.87	561.16	2.0

**Table 3: Parameter estimates for different regions.** See Eq. (1) for model parameters. All estimates are posterior medians. 75% and 95% credible intervals given for  $\tau$ , in days.  $\tau^*$  is the official last NPI date, see Table 1.

188 **Effect of late and early effect of NPIs on real-time assessment.** The success of non-pharmaceutical  
 189 interventions is assessed by health officials using various metrics, such as the decline in the growth  
 190 rate of daily cases. These assessments are made a specific number of days after the intervention began,  
 191 to accommodate for the expected serial interval<sup>14</sup> (i.e. time between successive cases in a chain of  
 192 transmission), which is estimated at about 4-7 days<sup>2</sup>.

193 However, a significant difference between the beginning of the intervention and the effective change in  
 194 transmission rates can invalidate assessments that assume a serial interval of 4-7 days and neglect the  
 195 late or early population response to the NPI. This is illustrated in Figure 5 using data and parameters  
 196 from Italy. Here, a lockdown is officially ordered on Mar 10 ( $\tau^*$ ), but its late effect on the transmission  
 197 dynamics starts on Mar 16 ( $\hat{\tau}$ ). If health officials assume the dynamics to immediately change at  $\tau^*$ ,  
 198 they will expect the number of cases be within the red lines (posterior predictions assuming  $\tau = \tau^*$ ).  
 199 This leads to a significant underestimation, which might be interpreted by officials as ineffectiveness  
 200 of NPIs, leading to further escalations. However, the number of cases will actually follow the blue  
 201 lines (posterior predictions using  $\tau = \hat{\tau}$ ), which corresponds well to the real data.

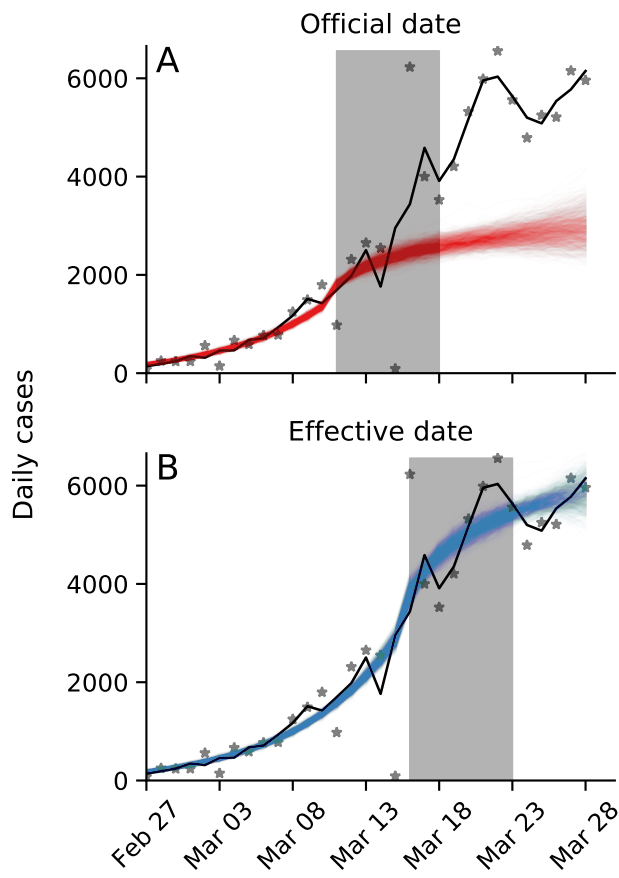


**Figure 5: Late effective start of NPIs leads to under-estimation of daily confirmed cases.** Real number of daily cases in Italy in black (markers: data, line: time moving average). Model posterior predictions are shown as colored lines (1,000 draws from the posterior distribution). Shaded box illustrates a serial interval of seven days. **(A)** Using the official date  $\tau^*$  for the start of the NPI, the model under-estimates the number of cases seven days after the start of the NPI. **(B)** Using the effective date  $\hat{\tau}$  for the start of the NPI, the model correctly estimates the number of cases seven days after the start of the NPI. Here, model parameters are estimates for Italy (Table 3).

202 **Discussion**

203 We have estimated the effective start date of NPIs in several geographical regions using an SEIR  
204 epidemiological model and an MCMC parameter estimation framework. We find examples of both  
205 late and early effect of NPIs (Figure 2).

206 For example, in Italy and Wuhan, China, the effective start of the lockdowns seems to have occurred  
207 more than five days after the official date (Figure 3). This difference might be explained by low  
208 compliance: In Italy, for example, the government intention to lockdown Northern provinces leaked  
209 to the public, resulting in people leaving those provinces<sup>2</sup>. Late effect of NPIs might also be due to  
210 the time required by both the government and the citizens to organize for a lockdown, and for the new  
211 guidelines to diffuse in the population.

212 In contrast, in most investigated countries (e.g., Spain and France), we infer reduced transmission  
213 rates even before official lockdowns were implemented (Figure 4). An early effective date might be  
214 due to adoption of social distancing and similar behavioral adaptations in parts of the population,  
215 maybe in response to increased risk perception due to domestic or international COVID-19-related  
216 reports. This finding may also suggest that severe NPIs, such as lockdowns, were unnecessary, and  
217 that less extreme measures adopted by the population could have been sufficient for epidemic control.  
218 These less extreme measures may have been implemented due to government recommendations, media  
219 coverage, and social networks, rather than official NPIs. Indeed, the evidence supports a change in  
220 transmission dynamics (i.e. a model with free  $\tau$ ) even for Sweden (Figure S3a), in which a lockdown  
221 was not implemented\*, suggesting that lockdowns may not be necessary if other NPIs are adopted  
222 early enough during the outbreak<sup>14</sup>.

223 Attempts to asses the effect of NPIs<sup>3;14</sup> generally assume a seven-day delay between the implementation  
224 of the intervention and the observable change in dynamics, due to the characteristic serial interval of  
225 COVID-19<sup>2</sup>. However, the late and early effects we have estimated can confuse these assessments and  
226 lead to wrong conclusions about the effects of NPIs (Figure 5).

227 We have found that the evidence supports a model in which the parameters change at a specific time  
228 point  $\tau$  over a model without such a change-point in 9 out of 12 regions (Table 2). It will be interesting  
229 to check if the evidence favors a model with *two* change-points, rather than one. Two such change-  
230 points could reflect escalating NPIs (e.g. school closures followed by lockdowns), an NPI followed by  
231 a relaxation of the intervention, or a mix of NPIs and other events, such as weather, or domestic and  
232 international events that affect risk perception.

233 As several countries (e.g. Austria, Israel) begin to relieve lockdowns and ease restrictions, we expect  
234 similar delays and advances to occur: in some countries people will begin to behave as if restrictions  
235 were eased even before the official date, and in some countries people will continue to self-restrict  
236 even after restrictions are officially removed.

237 **Conclusions.** We have estimated the effective start date of NPIs and found that they often differ from  
238 the official dates. Our results highlight the complex interaction between personal, regional, and global  
239 determinants of behavioral response to infectious disease. Therefore, we emphasize the need to further  
240 study variability in compliance and behavior over both time and space. This can be accomplished  
241 both by surveying differences in compliance within and between populations<sup>7</sup>, and by incorporating  
242 specific behavioral models into epidemiological models<sup>15;16;17</sup>.

---

\*Sweden banned public events on Mar 12, encouraged social distancing on Mar 16, and closed schools on Mar 18<sup>3</sup>.

243 **Acknowledgements**

244 We thank Lilach Hadany and Oren Kolodny for discussions and comments. This work was supported in part by  
245 the Israel Science Foundation 552/19 and 1399/17.

246 **References**

- [1] R. Li, *et al.*, *Science* (80-. ). p. eabb3221 (2020).
- [2] M. Gatto, *et al.*, *Proc. Natl. Acad. Sci.* p. 202004978 (2020).
- [3] S. Flaxman, *et al.*, *Imp. Coll. London* pp. 1–35 (2020).
- [4] M. R. Kaufman, F. Cornish, R. S. Zimmerman, B. T. Johnson, *J. Acquir. Immune Defic. Syndr.* **66**, 250 (2014).
- [5] A. G. Dunn, J. Leask, X. Zhou, K. D. Mandl, E. Coiera, *J. Med. Internet Res.* **17**, e144 (2015).
- [6] A. B. Wiyeh, S. Cooper, C. A. Nnaji, C. S. Wiysonge, *Expert Rev. Vaccines* **17**, 1063 (2018).
- [7] C. J. Atchison, *et al.*, *medRxiv* p. 2020.04.01.20050039 (2020).
- [8] L. E. Smith, *et al.*, *medRxiv* pp. 1–20 (2020).
- [9] C. M. Zipfel, S. Bansal, *medRxiv* pp. 1–13 (2020).
- [10] S. Pei, J. Shaman, *medRxiv* p. 2020.03.21.20040303 (2020).
- [11] J. Goodman, J. Weare, *Commun. Appl. Math. Comput. Sci.* **5**, 65 (2010).
- [12] D. Foreman-Mackey, D. W. Hogg, D. Lang, J. Goodman, *Publ. Astron. Soc. Pacific* **125**, 306 (2013).
- [13] A. Gelman, *et al.*, *Bayesian Data Analysis, Third Edition*, Chapman & Hall/CRC Texts in Statistical Science (Taylor & Francis, 2013).
- [14] N. Banholzer, E. V. Weenen, B. Kratzwald, A. Seeliger, *medRxiv* (2020).
- [15] E. P. Fenichel, *et al.*, *Proc. Natl. Acad. Sci. U. S. A.* **108**, 6306 (2011).
- [16] C. E. Walters, J. R. Kendal, *Theor. Popul. Biol.* **90**, 56 (2013).
- [17] R. F. Arthur, J. H. Jones, M. H. Bonds, M. W. Feldman, *bioRxiv* pp. 1–23 (2020).

## Supplementary Material

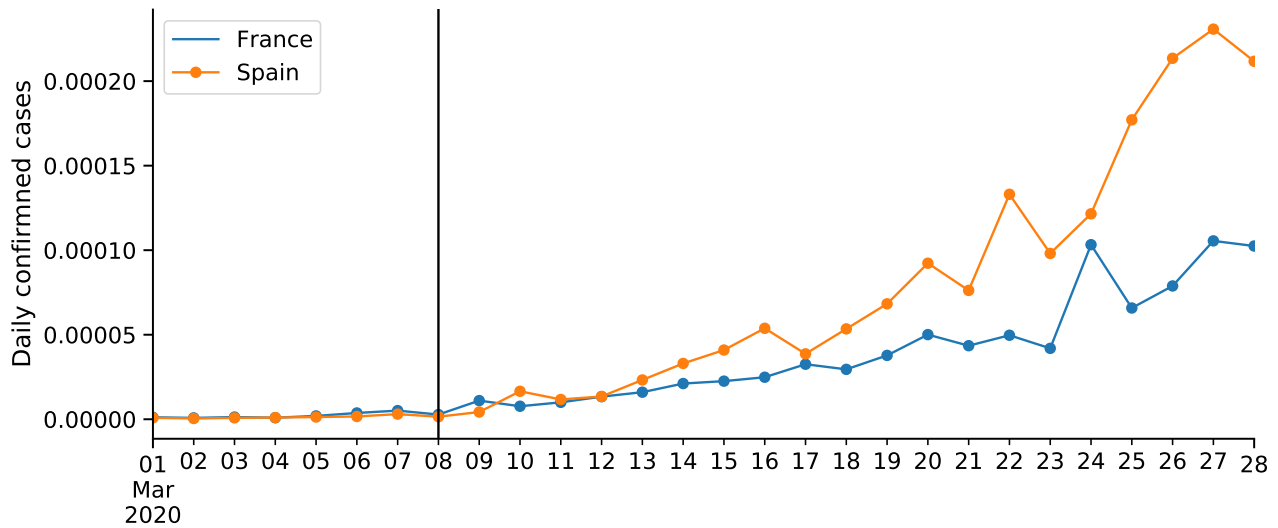


**Figure S1: COVID-19 confirmed cases in France and Spain.** Number of cases proportional to population size (as of 2018). Vertical line shows Mar 8, the effective start of NPIs  $\hat{\tau}$  in both countries.

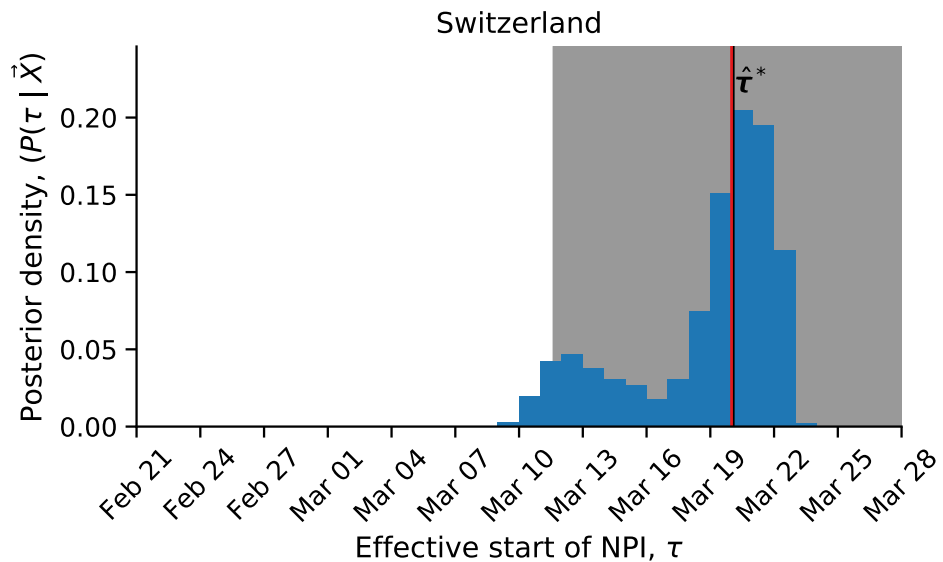
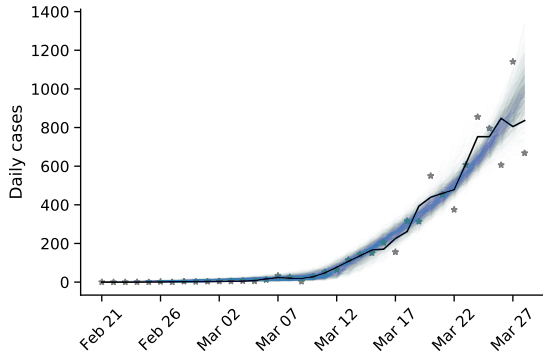
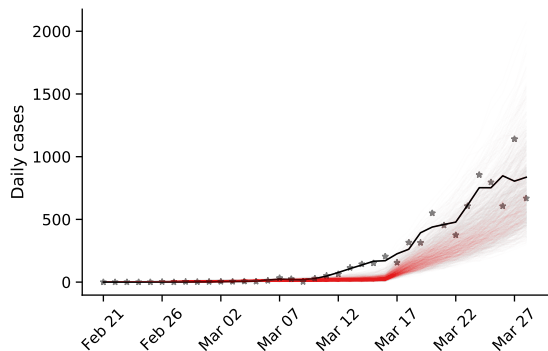
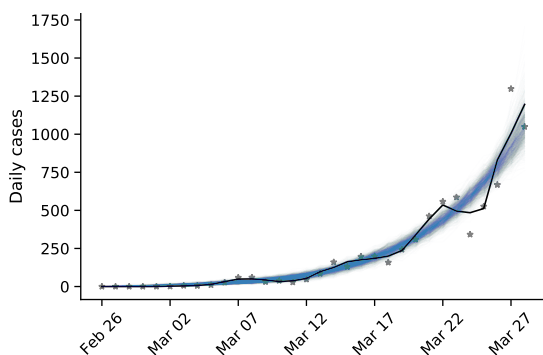
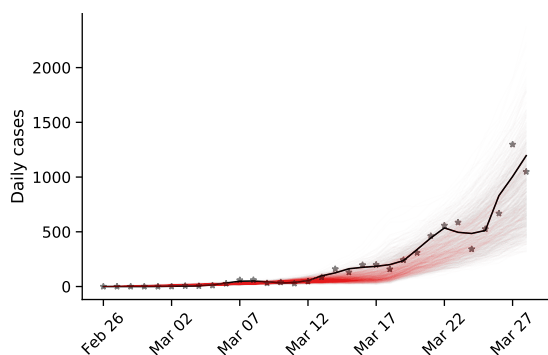


**Figure S2: Effective date of non-pharmaceutical interventions in Switzerland matches the official date**  
Posterior distribution of  $\tau$ , the effective start date of NPI, is shown as a histogram of MCMC samples. Red line shows the official last NPI date  $\tau^*$ . Black line shows the estimated  $\hat{\tau}$ . Shaded area shows a 95% credible interval (area in which  $P(|\tau - \hat{\tau}| < 2\sigma) = 0.95$ ).

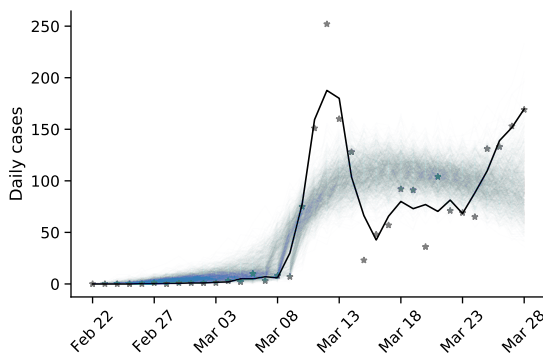
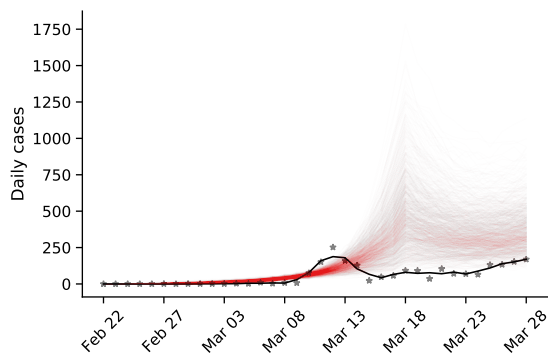
### Austria



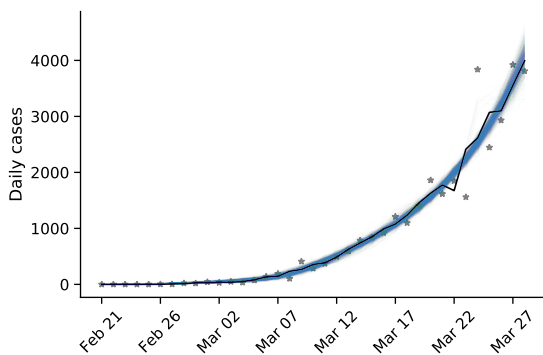
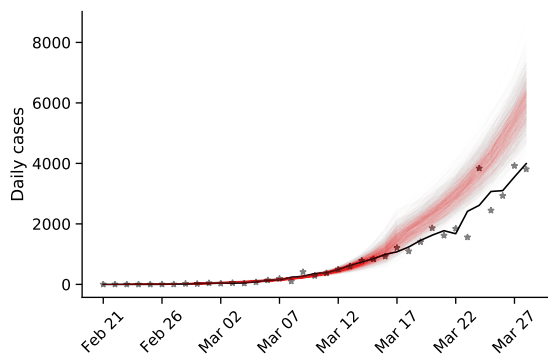
### Belgium



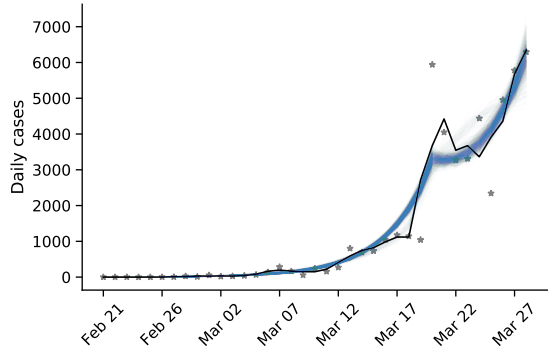
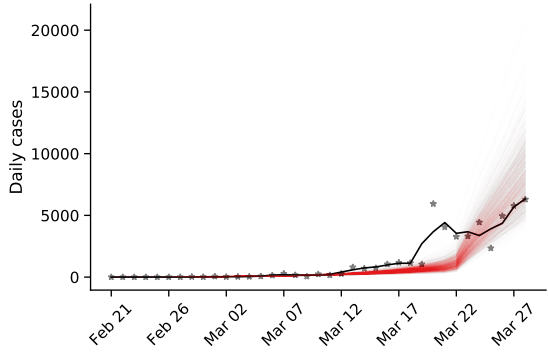
### Denmark



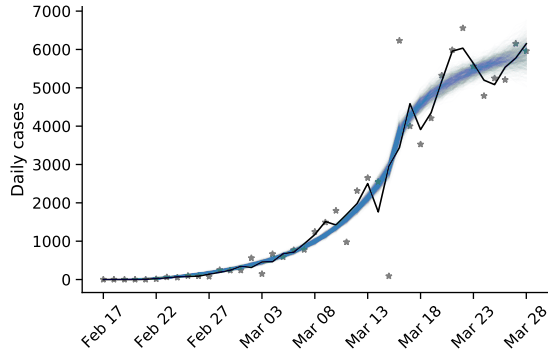
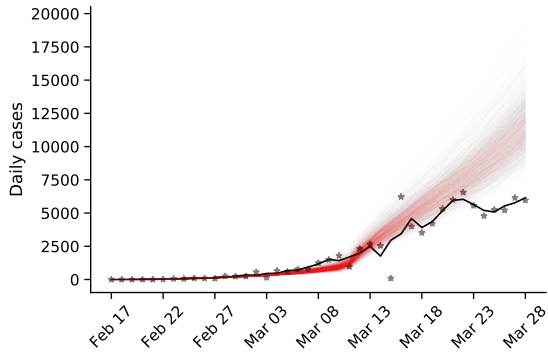
### France



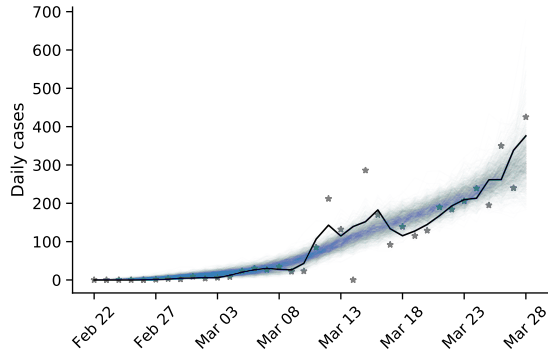
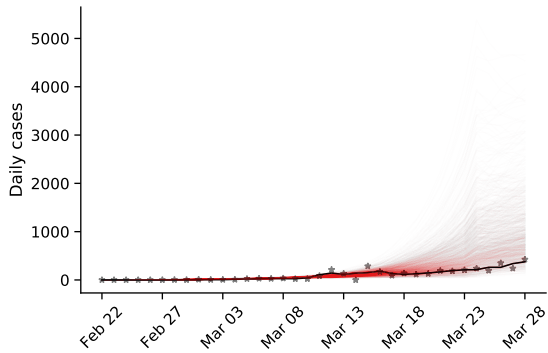
### Germany



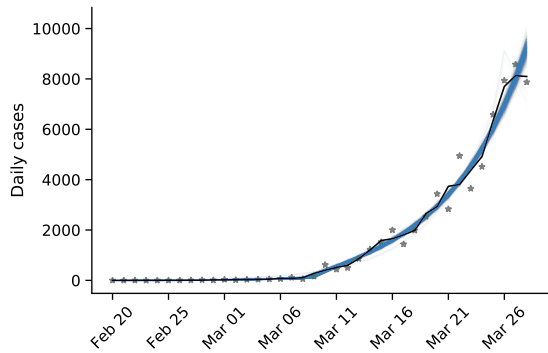
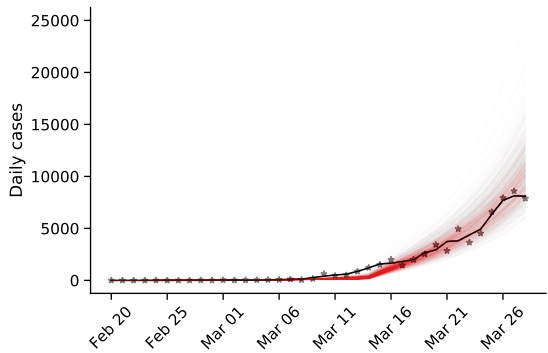
### Italy



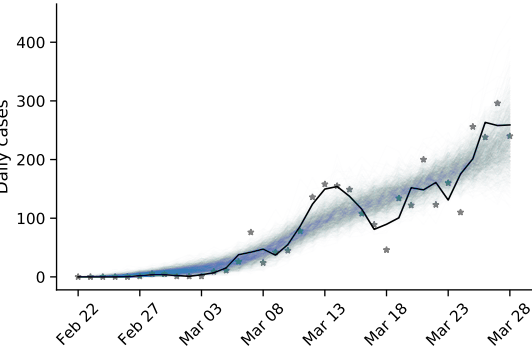
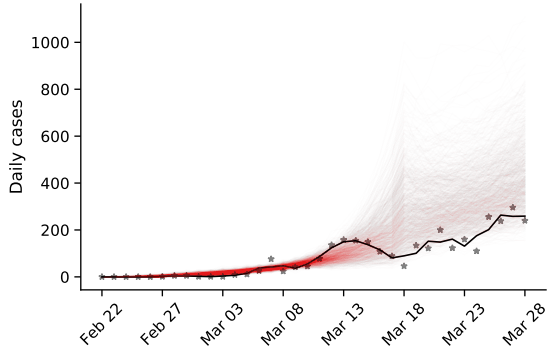
### Norway



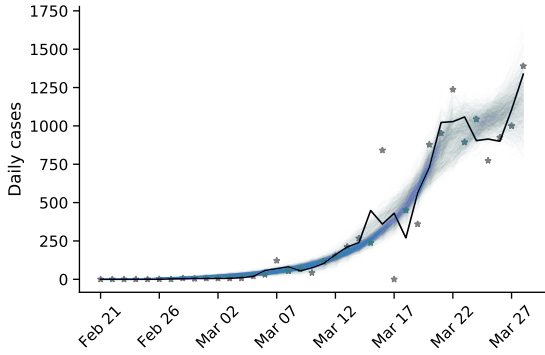
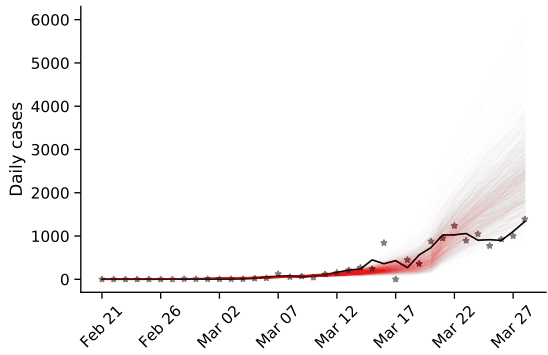
### Spain



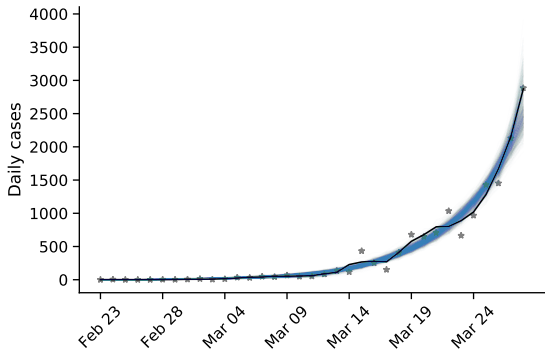
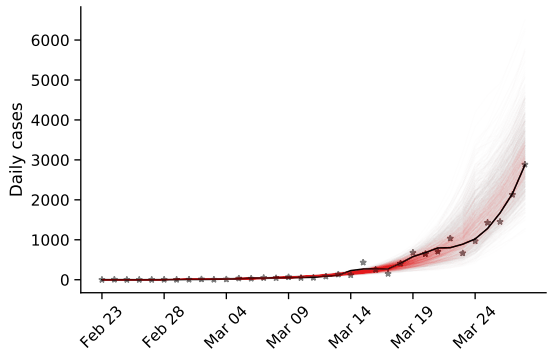
### Sweden



### Switzerland



### United Kingdom



### Wuhan, China

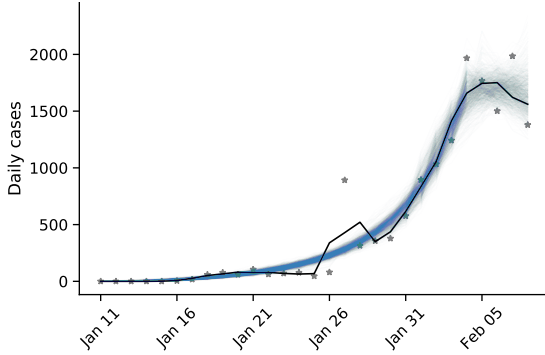
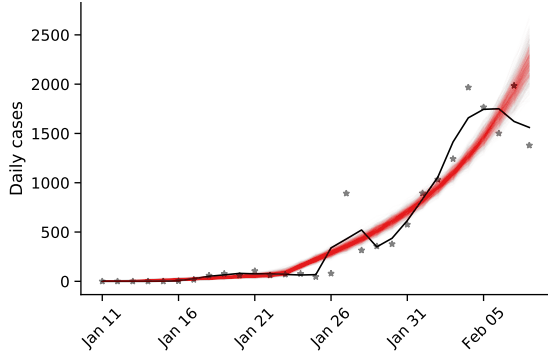


**Figure S3. Posterior prediction check plots** Markers represent data ( $\mathbf{X}$ ). Black line represent a smoothing of the data points using a Savitzky-Golay filter. Color lines represent posterior predictions from a model with fixed  $\tau$ , in red, and free  $\tau$ , in blue. These predictions are made by drawing 1,000 samples from the parameter posterior distribution and then generating a daily case count using the SEIR model in Eq. (1). Note the differences in the y-axis scale.